Dispersed Microfibril-Dominated Deformation and Fracture Behaviors of Linear Low Density Polyethylene/Isotactic Polypropylene Blends

Bing Na, Ruihua Lv, Zunxin Zhao

Department of Materials Science and Engineering, East China Institute of Technology, Fuzhou, Jiangxi 344000, People's Republic of China

Received 19 June 2006; accepted 10 November 2006
DOI 10.1002/app.25814
Published online in Wiley InterScience (www.interscience.wiley.com).

ABSTRACT: Linear low density polyethylene/isotactic polypropylene (LLDPE/iPP) blends, with oriented microfibrils of iPP dispersed in the nearly isotropic LLDPE matrix, has been prepared via melt extrusion drawing and subsequent thermal treatment at 160°C to melt LLDPE matrix. The presence of oriented microfibrils of iPP in the LLDPE/iPP blends not only promotes the homogenous deformation, with no drop of nominal stress around yield point, but also enhances the fracture toughness significantly. The specific Essential Work of Fracture w_e, which is a pure crack resistance parameter per ligament area unit, is 24.7 and 33.6 N/mm for the blends with 15 and 30 wt % microfibrils of iPP, respectively. Moreover, with the deduced deformation parameters, such as true yield stress and strain hardening modulus, the relationship between deformation parameters and fracture toughness is explored. It is demonstrated that the fracture toughness can be well correlated with the ratio of true yield stress to strain hardening modulus σ_{ty}/G, and either a decrease in yield stress or an increase in strain hardening can improve fracture toughness. © 2007 Wiley Periodicals, Inc. J Appl Polym Sci 104: 1291–1298, 2007

Key words: microfibril; fracture toughness; LLDPE/iPP blends

INTRODUCTION

Due to their relatively low cost and versatile properties, polyolefin have always attracted much attention as commercial materials.[1,2] Usually, two or more kinds of polyolefin have been blended to combine the attractive features of the constituent polymers and improve the deficient properties of one or both homopolymers. Among these systems, mixture of polyethylene (PE) and isotactic polypropylene (iPP) is the focus of investigation as results of the potential industrial applications of improving the impact strength and processability of the iPP and the environmental stress-cracking resistance of the PE.[3] In general, immiscible PE/iPP blends results in poor adhesion among its phases, coarse phase morphology, and thus poor mechanical properties.[4] In spite of numerous reports for improving the mechanical properties via either compatibilizer[5] or epitaxial growth among these two crystalline polymers,[6,7] that recent developing morphology control of dispersed phase via *in situ* fibrillation provides an effective way to enhance performances significantly because of the large capacity of load-bearing from oriented microfibrils in the isotropic matrix.[8–10] Major attention is paid to the improvement of mechanical performance, such as modulus and tensile strength, by adjusting preparation conditions. Besides modulus and tensile strength, however, the characteristics of deformation of such blends under tensile are less concerned in the past. Since the deformation of polymers is related to its microstructure,[11–13] it is expected that the presence of oriented microfibrils in the isotropic matrix can affect the yield, strain hardening, and fracture to large extent. On the other hand, though strength and toughness are two major concerned properties of polymer and its blends by researchers, there have little straightforward bridges between them yet. Therefore, to correlate deformation characteristics with fracture behaviors of such blends with microfibrils is somewhat instructive for further understanding the roles played by the microfibrils in the macroscopic mechanical properties. In this study, blends with oriented microfibrils of iPP dispersed in the linear low density polyethylene (LLDPE) matrix, prepared via melt extrusion drawing and subsequent thermal treatment at 160°C to melt LLDPE matrix, will be chosen to investigate the effect of oriented microfibrils on the deformation and fracture behavior. Moreover, with aid of Essential Work of Fracture (EWF) method, the fracture toughness of such blends

Correspondence to: B. Na (bingnash@163.com or bna@ecit.edu.cn).

Contract grant sponsor: Natural Science Foundation of Jiangxi, China; contract grant number: 0650009.
Contract grant sponsor: Doctoral Special Foundation of ECIT.

will be quantitatively determined. Finally, the relationship between deformation parameters, such as true yield stress and strain hardening modulus, and fracture toughness will be explored to some degree.

EXPERIMENTAL

Materials and sample preparation

LLDPE produced by Qilu Petrochemical (China), had a melt flow index (MFI) of 1.5 g/10 min and a melting point of about 125°C. iPP, supplied by the Dusanzi, had a MFI of 1 g/10 min and a melting point of about 165°C. Compositions with 15 and 30 wt % iPP in linear low density polyethylene/isotactic polypropylene (LLDPE/iPP) blends were selected. For convenience, sample code iPP-15 (30), labeled by the percentage of iPP, was adopted. Tapes with a thickness of 1 mm were first extruded, using a Haake counter-rotating twin-screw extruder with a barrel temperature of 160–200°C, and then drawn by a die drawing with the aid of rollers. After drawing, the tapes were reduced to about 0.3 mm in thickness corresponding to a drawing ratio of about eight (as given by the change in the cross-sectional area). Drawn tapes were thermally treated under a pressure of 2.5 MPa in a hot press for 30 min either at 160°C to melt PE only, referred to fibrillar samples, or at 200°C to melt both components, referred to isotropic samples. After then, samples were quickly transferred to a cold press for rapid cooling under a slight pressure.

Scanning electron microscope

Morphological observations were conducted by a JEOL scanning electron microscopy operated at 20 kV. Samples were first etched by toluene at its boiling point for 30 min to remove LLDPE component and then coated with gold.

Two-dimensional wide angle X-ray scattering

Two-dimensional wide angle X-ray scattering (2D WAXS) experiments were conducted, using a Rigaku Denki RAD-B diffractometer. The wavelength of the monochromated X-ray from Cu Kα radiation was 0.154 nm, and the transmission mode was used.

Uniaxial tensile tests

Specimens with dog-bone shape were punched from the fibrillar and isotropic samples, respectively. Tensile tests were conducted on an universal testing machine (WDT II) equipped with a 200 N load cell at room temperature, with a crosshead speed of 2 mm/min corresponding to an initial strain rate of 0.005 s^{-1}. As for the necked samples, the natural

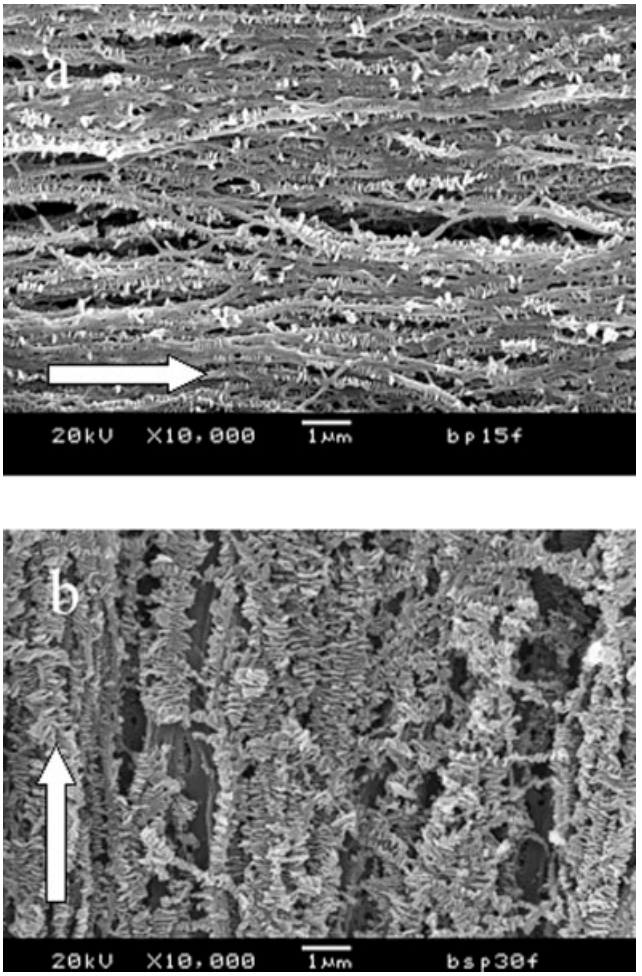

Figure 1 The phase morphology of dispersed iPP component in the fibrillar samples after thermally treatment at 160°C, with removing of LLDPE matrix by boiling toluene. (a) iPP-15 and (b) iPP-30. The arrows in the photographs indicate the original melt drawing direction.

draw ratio λ_n and draw ratio at break λ_f were determined from the separation of ink marks at regular 1-mm intervals preprinted on the specimens, with the aid of a CCD camera interfaced with the computer controlling the testing machine. This setup could synchronize the data acquisition of mechanical testing with image acquisition of the CCD camera. Moreover, the CCD camera, with a resolution of 1280 × 1024 pixel, was additionally interfaced with a tunable magnification lens, which makes it possible to *in situ* accurately measure the draw ratio during testing. The experimental results were the average of over five specimens.

Fracture tests

The EWF tests were performed by the same setup as uniaxial tensile tests, at room temperature and with a crosshead speed of 2 mm/min. Deeply double edge-notched samples were prepared by cutting the

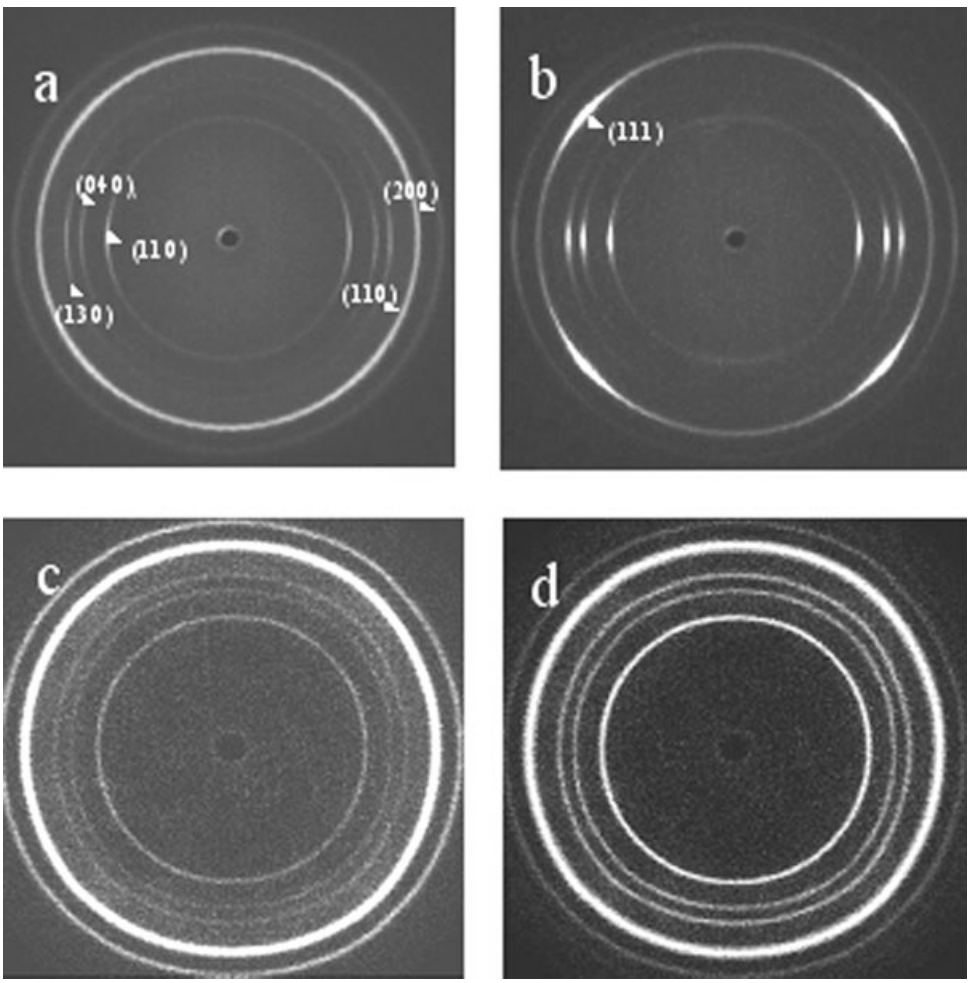

Figure 2 2D WAXS patterns of fibrillar samples iPP-15 (a) and iPP-30 (b) after thermal treatment at 160°C. The original melt extrusion drawing direction is vertical. For comparison, those of isotropic samples iPP-15 (c) and iPP-30 (d) after thermal treatment at 200°C are also included.

fibrillar and isotropic sheets into rectangular strip with a gauge length of 10 mm and a width of 10 mm. Initial notches were made perpendicularly to the tensile direction with a fresh razor blade. For meeting the requirements of plane stress, the ligament lengths of specimens were varied between 1 and 4 mm. The ligament lengths before testing were accurately measured with aid of the CCD camera mentioned earlier. Moreover, with this special setup a direct correlation of the two-dimensional deformation state with characteristic points of the load-displacement curve was possible. The load-displacement curves were recorded, and the absorbed energy was calculated by computer integration of the loading curves.

RESULTS AND DISCUSSION

Initial structure

By introducing of external stress during melt drawing, dispersed iPP component in the LLDPE/iPP blends could be deformed to some extent.[8–10,14] Moreover, the morphology of dispersed iPP component formed during the melt extrusion drawing could survive thermal treatment at 160°C, since it is lower than the melting point of iPP component. Figure 1 is the typical phase morphology of dispersed iPP component in the fibrillar samples after etching by boiling toluene to remove the LLDPE matrix. Evidently, numerous microfibrils are in fact formed along original drawing direction in both compositions studied. Note that removing LLDPE matrix may disturb the position of iPP microfibrils during sample preparation for morphology observation since the iPP component is minor in the blends. Moreover, shish-kebab structure, resulted from stress-induced crystallization during melt drawing,[15–17] can also be distinguished after removing of the amorphous part of iPP component by boiling toluene. The survived anisotropic structure of iPP component in the fibrillar samples is further demonstrated by the results of 2D WAXS shown in Figure 2. From inner

outward, the lattice planes are the (110), (040), (130) of iPP component and (110), (200) of LLDPE matrix, respectively. The reflections of (hk0) lattice planes of iPP component are all concentrated at the equator, from which molecular orientation of iPP component along original melt drawing direction can be deduced. The calculated Herman's orientation factor of (040) lattice plane of iPP component is −0.16 and −0.22 for iPP-15 and iPP-30, respectively. Moreover, the nearly isotropic reflections of (110) and (200) lattice planes indicate that the dominant morphology of LLDPE matrix is random, which confirm that thermal treatment at 160°C is enough to melt LLDPE matrix. Note that there has somewhat epitaxial growth between microfibrils of iPP and LLDPE matrix,[6,7] especially in the fibrillar sample iPP-30 [Fig. 2(b)], indicated by the reflection of (110) lattice plane of LLDPE overlapping with that of (111) lattice plane of iPP, but its fraction is no more than 20% in both compositions by calculation.[18] From the earlier results, therefore, a structure with dispersed microfibrils of iPP in the nearly isotropic LLDPE matrix can be constructed. For comparison, the results of 2D WAXS patterns from isotropic samples are also shown in Figure 2. Apparently, after thermal treatment at 200°C the structure formed during the original melt extrusion drawing has been destroyed completely and thus isotropic scatterings from all lattice planes of two polymers are presented in both compositions.

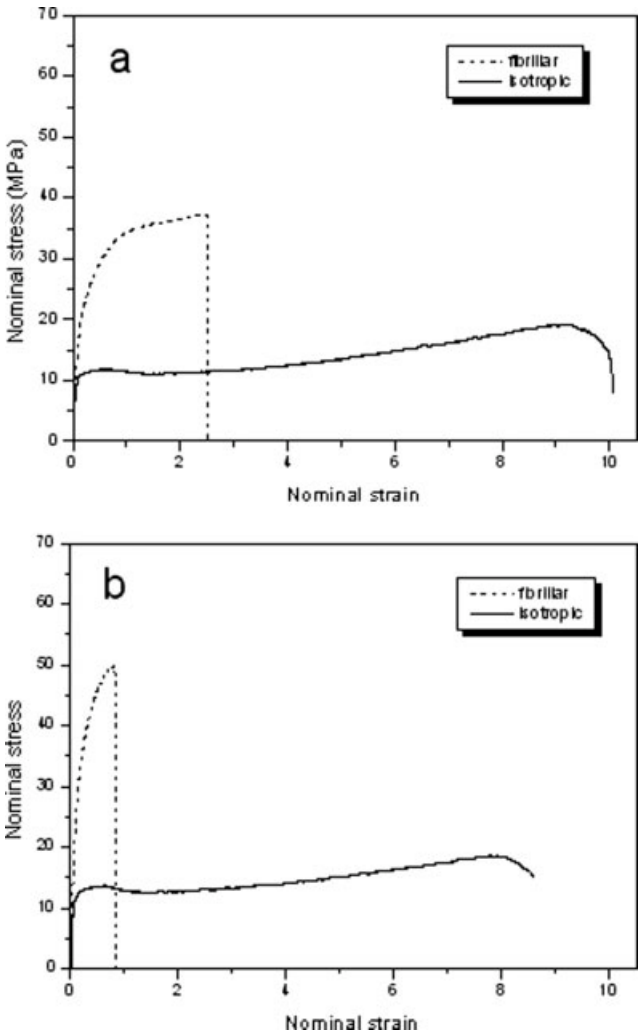

Figure 3 The nominal stress strain curves, obtained at a nominal strain rate of 2 mm/min, of both fibrillar and isotropic samples, iPP-15 (a) and iPP-30 (b).

Uniaxial tensile behavior

The uniaxial tensile behavior of both fibrillar and isotropic samples is presented in Figure 3. As expected, inhomogeneous deformation, demonstrated by the drop of load around yield point, is brought up for both compositions of isotropic samples thermally treated at 200°C. This situation is similar to the samples of PE/iPP blends without any orientation.[19] It is the fact in this case, since thermal treatment at 200°C can destroy any molecular orientation induced by original melt extrusion drawing (see Fig. 2), with consideration of the (equilibrium) melting point of PE and iPP. After yield, a stable neck is formed in both compositions until fracture. Stable necking provides an effective way to obtain the ratio of true yield stress σ_{ty} to strain hardening modulus G as long as the natural draw ratio in the neck λ_n is known.[20] The reason is that a stable neck is formed when equilibrium is reached between the load transferred in the neck and that in the undeformed zone. At this point the load in the neck will be large enough to induce yield in the adjacent undeformed material and the natural draw ratio in neck λ_n is shown to be related to the true yield stress σ_{ty} and strain hardening modulus G as follows:

$$\sigma_{ty}A_0 = \left[\sigma_{ty} + G\left(\lambda_n^2 - \frac{1}{\lambda_n}\right)\right]\frac{A_0}{\lambda_n} \quad (1)$$

$$\frac{\sigma_{ty}}{G} = \left(\lambda_n^2 - \frac{1}{\lambda_n}\right)/(\lambda_n - 1) \quad (2)$$

where A_0 is the cross-sectional area of undeformed sample. The results of calculated σ_{ty}/G for both compositions of isotropic samples are reproduced in Table I. Moreover, with the value of true yield stress σ_{ty}, the strain hardening modulus G can be deduced. However, the gain of true yield stress σ_{ty} is not straightforward due to necking[21] and it could only be estimated from the stress level in the middle of the transition from the initial elastic region to the yield point.[20] The calculated strain hardening modulus looks reasonable and is comparable with the

TABLE I
The Intrinsic Deformation Parameters, Deduced from Uniaxial Tensile Tests, of Both Isotropic and Fibrillar Samples

		λ_n	G (MPa)	σ_y (MPa)	σ_y/G	λ_f	σ_{tf} (MPa)
Fibrillar	iPP-15	–	7.1 (0.9)	15.1 (1.2)	2.1 (0.4)	3.4 (0.3)	131.3 (10.5)
	iPP-30	–	20.3 (1.8)	25.2 (2.1)	1.2 (0.2)	1.8 (0.2)	90.7 (13.7)
Isotropic	iPP-15	4.7 (0.5)	1.6 (0.3)	9.3 (0.8)	5.9 (0.5)	8.8 (0.8)	190.1 (22.4)
	iPP-30	5.0 (0.4)	1.7 (0.3)	10.9 (1.1)	6.2 (0.4)	8.5 (0.9)	167.6 (19.8)

The number in the brackets is the standard deviation.

value of pure LLDPE. With the value of draw ratio at break λ_f and nominal fracture stress σ_{nf}, moreover, the true fracture stress σ_{tf} can be also estimated. These results are also included in Table I.

Different from the isotropic ones, homogenous extension, with characteristics of no fall of drop around yield point, is realized in both compositions of fibrillar samples. Thanks for the homogenous deformation, strain hardening modulus G can be obtained with plotting of true stress $\sigma_{true} = \sigma_n \times \lambda$ as a function of $\lambda^2 - 1/\lambda$, which has been well demonstrated elsewhere.[21,22] True yield stress σ_{ty} can also be deduced from the maximum curvature on the true stress–strain curves with construction of true stress $\sigma_{true} = \sigma_n \times \lambda$ versus true strain $\varepsilon = \ln \lambda$, where σ_n is the nominal stress and λ is the draw ratio. Both calculated G and σ_{ty} are listed in the Table I, where the value of σ_{ty}/G is also included.

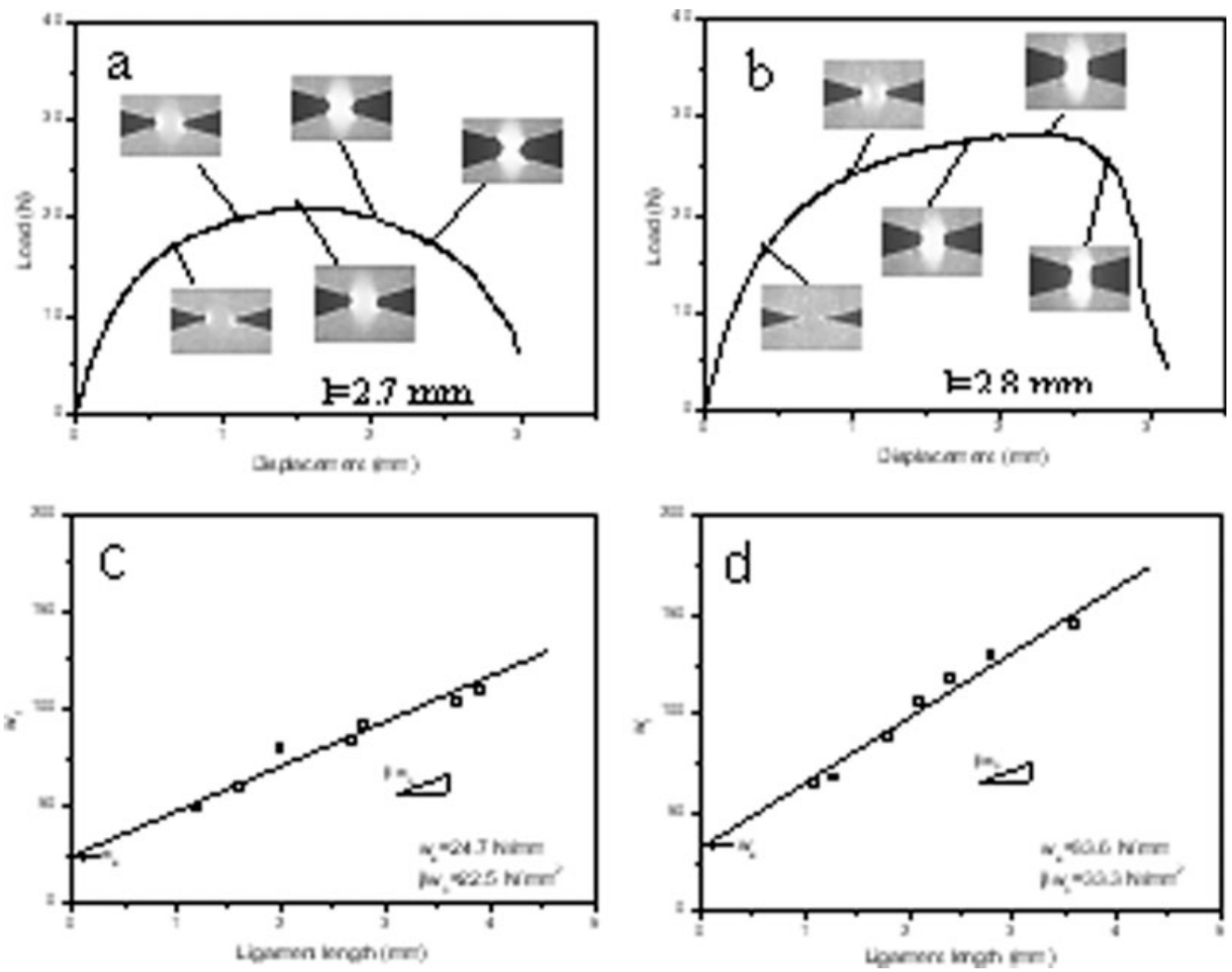

Figure 4 Typical load displacement curve (a, b) and deduced specific EWF w_e (c, d) of fibrillar samples iPP-15 (a, c) and iPP-30 (b, d). The initial notches are perpendicular to the original melt extrusion direction.

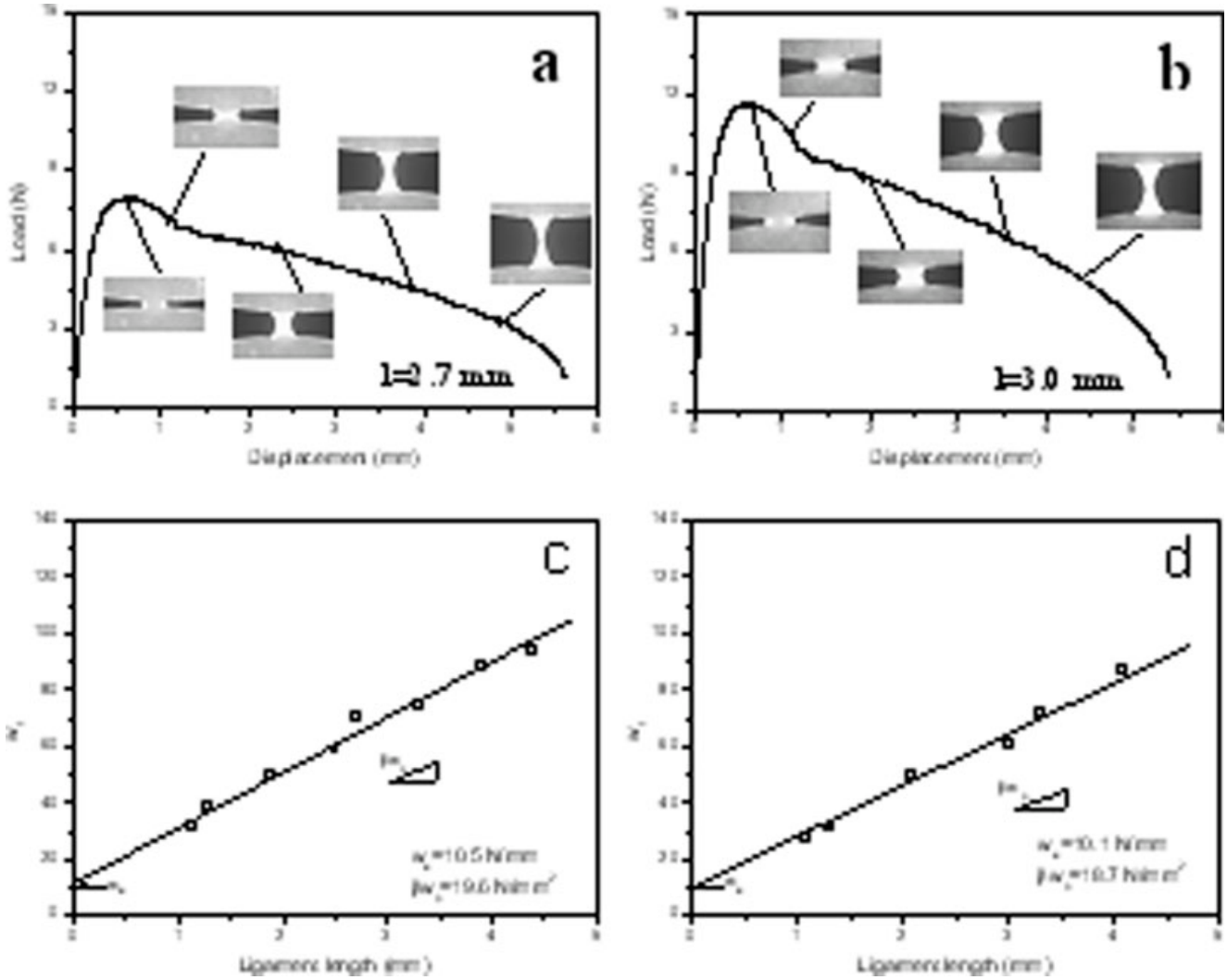

Figure 5 Typical load displacement curve (a, b) and deduced specific EWF w_e (c, d) of isotropic samples iPP-15 (a, c) and iPP-30 (b, d). The initial notches are perpendicular to the original melt extrusion direction.

Note that the values of G and σ_{ty} of fibrillar samples are much higher, while compared with those of isotropic PE listed in the literature.[21,22] They, however, are consistent with those of oriented PE with shish structure.[20] Apparently, the value of σ_{ty}/G of samples deformed homogenously drops down to three or lower, which is in agreement with Consedere's condition.[22] Moreover, the steeper increasing of stress after yield, the lower is the value of σ_{ty}/G. The microfibrils of iPP component dispersed in the isotropic PE matrix could be responsible for the homogenous extension, since oriented microfibrils of iPP can effectively bear the load after yield and promote the strain hardening to occur in advance. Moreover, the true fracture stress of both fibrillar samples is calculated with knowledge of the value of draw ratio at break λ_f. Apparently, the true fracture stress is decreased with the content of microfibrils.

Fracture behavior

The EWF method, which emphasizes the crack initiation and propagation, has been extensively adopted to evaluate the fracture toughness of ductile polymer films or tapes.[23,24] Figure 4 is the results of EWF tests of both compositions of fibrillar samples with the initial notches perpendicular to its original melt extrusion drawing direction. With help of the CCD camera, the process of deformation is monitored and can be directly related to the points on the load displacement curve. Apparently, the plastic zone is formed due to amplification of stress close to crack tip before crack propagation occurs, which confirms the precondition of application of EWF concept.[24] While maximum flow stress is reached, crack propagation sets in gradually until ultimate fracture. Comparing the load displacement curve and related photographs, it is evident that the crack initiation

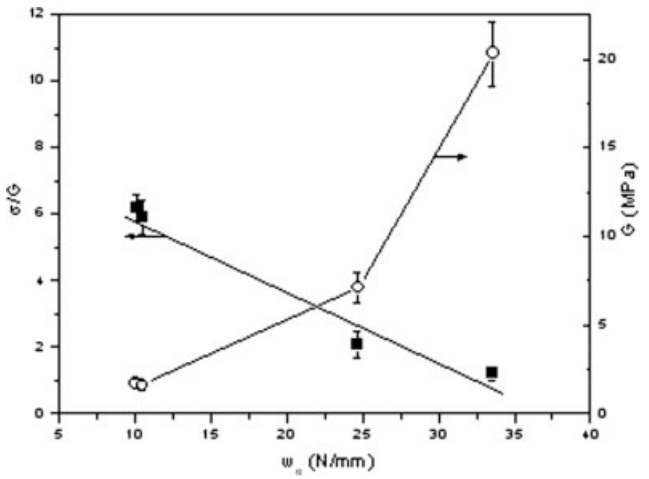

Figure 6 The relationship between specific EWF w_e and strain hardening modulus G and the ratio of true yield stress to strain hardening modulus σ_{ty}/G, respectively.

and propagation is much easier in the fibrillar sample iPP-15. Plotting of the specific work of fracture w_f as a function of ligament lengths could yield specific EWF w_e, which is also shown in Figure 4. The deduced specific EWF w_e is 24.7 and 33.6 N/mm for fibrillar sample iPP-15 and iPP-30, respectively. It is indicated that the fracture toughness is increased with the content of iPP microfibrils, which is consistent with the changing of deformation state manifested by the photographs.

The typical load displacement curve of both compositions of isotropic samples is presented in Figure 5, where images related to the various deformation states are also included. Clearly the crack initiation and propagation are much easier in the isotropic samples, which is further demonstrated by the deduced specific EWF w_e. It is 10.5 and 10.1 N/mm for isotropic sample iPP-15 and iPP-30, respectively.

From the earlier results, it is obvious that the fracture toughness of fibrillar and isotropic samples of LLDPE/iPP blends can be effectively determined with aid of EWF method. The specific EWF w_e, which is a pure crack resistance parameter per ligament area unit, is varied with respect to phase morphology and the content of iPP component in the LLDPE/iPP blends. It is apparent that incorporation of iPP microfibrils in the LLDPE matrix can enhance the fracture toughness to large extent in addition to increasing of yield strength, which is similar to the results of flow-oriented samples.[20,25] Moreover, a close inspection of the relationship between specific EWF w_e of all samples and the deformation parameters included in Table I could yield some instructive results. It is frequent to state that the yield stress is the decisive factors of fracture toughness, and reducing of the yield stress to delay reaching the fracture strength is an effective way to improve the fracture toughness.[26] However, in this case the earlier argument seems to be unsuitable, since the fracture toughness is increased with true yield stress. It indicates that the yield stress seems to be a nondecisive factor determining the fracture toughness of LLDPE/iPP blends. Further analysis demonstrate that the relationship between w_e and σ_{ty}/G seems to be more straightforward. Such a plot of σ_{ty}/G as a function of essential EWF w_e is shown in Figure 6, where the relationship between G and w_e is also included. It means that the fracture toughness of LLDPE/iPP blends is mostly resulted from the coeffect of yield and strain hardening. In other words, the fracture toughness of samples is dependent on the ratio between intrinsic yield stress and strain hardening modulus, and either a decrease in yield stress or an increase in strain hardening can enhance fracture toughness, which is similar to the situation in tension.[20]

CONCLUSIONS

The deformation and fracture of LLDPE/iPP blends with oriented microfibrils of iPP dispersed in the LLDPE matrix have been well demonstrated by the uniaxial and fracture tests. With the deduced deformation parameters, such as true yield stress, strain hardening modulus and true fracture stress, and fracture toughness, the role of the oriented microfibrils of iPP in the deformation and fracture of such blends is disclosed. Moreover, the relationship between deformation parameters and fracture toughness is well established, which give a deep insight into the fracture and toughness of polymer blends.

References

1. Flaris, V.; Wasiak, A.; Wenig, W. J Mater Sci 1993, 28, 1685.
2. Dumoulin, M. M.; And Carreau, P. J. Polym Eng Sci 1987, 27, 1627.
3. Teh, J. W.; Rudin, A.; Keung, J. C. Adv Polym Technol 1994, 13, 1.
4. Krause, S. Polymer Blends; Academic Press: New York, 1978; Vol. 1.
5. Blom, H. P.; Rudin, A. J Appl Polym Sci 1996, 61, 959.
6. Gross, B.; Petermann, J. J Mater Sci 1984, 19, 105.
7. Petermann, J.; Broza, G.; Rieck, G. J Mater Sci 1987, 22, 1477.
8. Li, J. X.; Wang, Q.; Chan, C. M.; Wu, J. S. Polymer 2004, 45, 5719.
9. Li, J. X.; Wu, J. S.; Chan, C. M. Polymer 2000, 41, 6935.
10. Sherman, E. S. J Mater Sci 1984, 19, 4014.
11. Butler, M. F.; Donald, A. M. Macromolecules 1998, 31, 6234.
12. Seguela, R.; Elkoun, S.; Gaucher-Miri, V. J Mater Sci 1998, 33, 1801.
13. Butler, M. F.; Donald, A. M.; Ryan, A. J. Polymer 1997, 38, 5521.

14. Huneauh, M. A.; Utracki, I. A. Polym Eng Sci 1995, 35, 115.
15. Kumaraswamy, G.; Issaian, A. M.; Kornfield, J. A. Macromolecules 1999, 32, 7537.
16. Somani, R. H.; Hsiao, B. S.; Yang, L. Macromolecules 2002, 35, 9096.
17. Pogodina, N. V.; Lavrenko, V. P.; Winter, H. H. Polymer 2001, 42, 9031.
18. Na, B.; Wang, K.; Zhao, P.; Zhang, Q.; Fu, Q. Polymer 2005, 46, 5258.
19. Finlay, J.; Sheppard, S.; Hill, M. J.; Barham, P. J. J Polym Sci Part B: Polym Phys 2001, 39, 1404.
20. Schrauwen, B. A. G.; Breemen, L. C. A.; Spoelstra, A. B.; Govaert, L. E.; Peters, G. W. M.; Meijer, H. E. H. Macromolecules 2004, 37, 8618.
21. Hiss, R.; Hobeika, C. L.; Strobl, G. Macromolecules 1999, 32, 4390.
22. Haward, R. N. Macromolecules 1993, 26, 5860.
23. Wu, J.; Mai, Y. W. Polym Eng Sci 1996, 36, 2275.
24. Lach, R.; Schneider, K.; Weidisch, R.; Janke, A.; Knoll, K. Eur Polym Mater 2005, 41, 383.
25. Galeski, A. Prog Polym Sci 2003, 28, 1643.
26. Bartczak, Z.; Argon, A. S.; Cohen, R. E.; Weinberg, M. Polymer 1999, 40, 2331.